MTL TR 89-98

AD

QUALITY EVALUATION OF COATINGS BY AUTOMATIC SCRATCH TESTING

KIRIT J. BHANSALI
U.S. ARMY MATERIALS TECHNOLOGY LABORATORY
METALS RESEARCH BRANCH

THEO Z. KATTAMIS
INSTITUTE OF MATERIALS SCIENCE
UNIVERSITY OF CONNETICUT, STORRS, CT

November 1989

US ARMY
LABORATORY COMMAND
MATERIALS TECHNOLOGY LABORATORY

U.S. ARMY MATERIALS TECHNOLOGY LABORATORY
Watertown, Massachusetts 02172-0001

The findings in this report are not to be construed as an official Department of the Army position, unless so designated by other authorized documents.

Mention of any trade names or manufacturers in this report shall not be construed as advertising nor as an official indorsement or approval of such products or companies by the United States Government.

DISPOSITION INSTRUCTIONS

Destroy this report when it is no longer needed.
Do not return it to the originator.

UNCLASSIFIED

SECURITY CLASSIFICATION OF THIS PAGE *(When Data Entered)*

REPORT DOCUMENTATION PAGE		READ INSTRUCTIONS BEFORE COMPLETING FORM
1. REPORT NUMBER MTL TR 89-98	2. GOVT ACCESSION NO.	3. RECIPIENT'S CATALOG NUMBER
4. TITLE *(and Subtitle)* QUALITY EVALUATION OF COATINGS BY AUTOMATIC SCRATCH TESTING		5. TYPE OF REPORT & PERIOD COVERED Final Report 6. PERFORMING ORG. REPORT NUMBER
7. AUTHOR(s) Kirit J. Bhansali and Theo Z. Kattamis*		8. CONTRACT OR GRANT NUMBER(s)
9. PERFORMING ORGANIZATION NAME AND ADDRESS U.S. Army Materials Technology Laboratory Watertown, Massachusetts 02172-0001 SLCMT-EMM		10. PROGRAM ELEMENT, PROJECT, TASK AREA & WORK UNIT NUMBERS
11. CONTROLLING OFFICE NAME AND ADDRESS U.S. Army Laboratory Command 2800 Powder Mill Road Adelphi, Maryland 20783-1145		12. REPORT DATE November 1989 13. NUMBER OF PAGES 18
14. MONITORING AGENCY NAME & ADDRESS *(if different from Controlling Office)*		15. SECURITY CLASS. *(of this report)* Unclassified 15a. DECLASSIFICATION/DOWNGRADING SCHEDULE

16. DISTRIBUTION STATEMENT *(of this Report)*

Approved for public release; distribution unlimited.

17. DISTRIBUTION STATEMENT *(of the abstract entered in Block 20, if different from Report)*

18. SUPPLEMENTARY NOTES

*Institute of Materials Science, University of Connecticut, Storrs, CT 06269-1136.

19. KEY WORDS *(Continue on reverse side if necessary and identify by block number)*

Coatings
Ceramic coatings
Adhesion
Acoustic emission
Tribology
Wear resistant coatings

20. ABSTRACT *(Continue on reverse side if necessary and identify by block number)*

(SEE REVERSE SIDE)

DD FORM 1 JAN 73 1473 EDITION OF 1 NOV 65 IS OBSOLETE

UNCLASSIFIED

SECURITY CLASSIFICATION OF THIS PAGE *(When Data Entered)*

Block No. 20

ABSTRACT

The soundness and comparative quality of various coatings were evaluated with a CSEM-Revetest automatic scratch tester. These coatings were: TiB_2 on MP35N alloy, TiN on PH 17-4 steel, $(Al_2O_3\text{-}SiO_2\text{-}Cr_2O_3)$ on PH 17-4 steel, and plasma-enhanced CVD-processed SiC on 4340 low alloy steel. During scratch testing, the acoustic emission signal intensity, the frictional or tangential force, and the friction coefficient were plotted versus load, as well as time at various constant loads. Scratch test results were correlated with coating microstructure which was investigated by optical and scanning electron microscopy (SEM). Significant difference in quality and soundness was detected for TiN coatings processed by two different methods. This difference was confirmed by abrasive wear resistance measurements.

CONTENTS

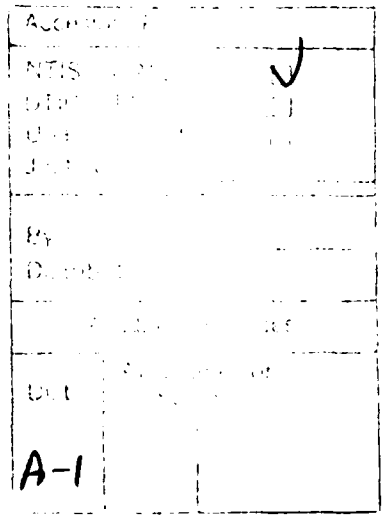

INTRODUCTION

The U.S. Army Laboratory Command (LABCOM) and the U.S. Army Armament, Munitions, and Chemical Command (AMCCOM) have been developing a new high performance gun that utilizes a liquid propellant (LP) charge. This gun, generally referred to as the LP gun, offers a number of advantages over conventional guns. A proprietary seal design and combustion technology, known as regenerative technology, allows controlled combustion of a hydroxyl ammonium nitrate (HAN)-based monopropellant to provide superior ballistic performance. This new design. however, offers significant challenges for materials in general, and seal materials in particular. The corrosive nature of the propellant is not only detrimental to a material's durability, but ensuing corrosion products quite often affect the performance of the propellant. Extreme high temperatures and pressures in combination with thermomechanical fatigue experienced by seals demand performance that no single material can satisfactorily deliver. Consequently, emerging coating technology is being considered for mitigating damage under these severe conditions. Coating processes that can satisfy the need to preserve the heat treatment, the structure, and the surface finish of the substrate were given priority. Accordingly, thin films deposited by a number of vapor deposition processes were considered. A number of candidate coatings were applied on the substrate structural materials, usually PH 17-4 steel. These samples were first screened for compatibility with the HAN propellant and the successful candidates were considered for the seals application.

Certain thin films processed by physical vapor deposition (PVD) or chemical vapor deposition (CVD) are extensively used industrially because of their remarkable specific resistance to numerous degradation processes such as abrasion, erosion, microwelding and galling, corrosion, high temperature oxidation and radiation damage, their lubricity and resistance to sticking, as well as their magnetic and dielectric properties. Such coatings as TiC, TiN, Ti(C,N), $Cr_{23}C_2$, and Al_2O_3 are commonly used on cemented carbide cutting inserts, high speed steel tools and roller bearing elements operating under severe service conditions of either very high or low temperatures, corrosive environments, and where lubrication may be absent. Reduced friction characteristics of TiN coatings enable drilling speeds and feeding velocities to be doubled or tripled without significant tool wear.[1,2] Coatings are also used for electrical contacts, body implants, watches, and jewelry. Deposition of TiN coatings through PVD in vacuum, using evaporation of Ti with an electron beam or arc discharge, as well as sputtering or atomic bombardment to atomize the target material[3] often leads to poor adhesion to the substrate. This problem can be overcome by plasma-enhanced processes such as PEPVD or PECVD.

It was realized, very early on, that in addition to providing chemical compatibility, the coating process itself played a significant role in the eventual performance of the coating in a 30-mm LP gun dedicated for seal testing. Hence, a screening test for evaluating variations in both the coating process and the resultant coating quality was needed. The structure, integrity, properties, and performance of films depend upon adhesion to the substrate. Sufficiently good intrinsic cohesive strength of the coating and adhesive strength to the substrate material yield considerably increased tool life and performance of work pieces. Three critical coating properties are: (1) elastic strain limit, which is an important parameter related to wear[4,5] where high elastic strains to inhibit crack initiation and propagation are necessary in order to

1. THORNLEY, R. H., and UPTON, D. P. presented at Fintech Symposium, Espoo, Finland, March 17-21, 1986.
2. THOMAS, A., and THOMSON, P. presented at the Plasma-Assisted Coatings Technology Seminar (Cutting Tools), National Center of Tribology, U.K., June 11, 1986.
3. MATTHEWS, A. *Surface Engineering* v. 1, 1985, p. 93.
4. OBERLE, T. S. J. of Met. v. 3, 1958, p. 438.
5. SUH, N. P. *Wear.* v. 25, 1973, p. 111.

reduce wear; (2) hardness, which is a dominant property influencing all forms of wear (abrasive, adhesive, fretting) – most metal (Al, Ti, W, Hf) nitrides are hard and so are carbides, borides, and oxides; and (3) hot hardness, which is particularly important for cutting tools. Ceramic coatings deposited by PVD or CVD techniques should, therefore, be ideal with additional advantages of: (1) good resistance to abrasion; (2) low friction coefficient, hence good resistance to adhesive wear and greatly reduced possibility of seizure, galling, and scuffing; (3) low thermal conductivity, providing good thermal barriers against bulk tool heating; (4) good corrosion resistance, such as TiC in sea water; and (5) attractive cosmetic gold color of nitrides, such as TiN, ZrN, and HfN.

Coatings deposited by PVD or CVD must meet the following requirements: (1) good substrate bonding, with no spalling even when the coated substrate is bent by 90°. (A high adhesion value can be achieved by appropriately heating[6] the substrate during deposition. Good coatings of commercial TiN exhibit a very fine grain size and a high dislocation density.); (2) controllable surface topography; (3) uniform coating thickness; (4) high structural integrity; and (5) reproducibility through computer-controlled vacuum processing. Most of the CVD- or PVD-processed thin, hard coatings have a low friction coefficient (μ^*) against themselves or steel and are very wear resistant.[7-11] Unlubricated bearings with coated balls or rings have been used very successfully in high temperature applications[12] or in the high vacuum of outer space.[13]

The interfacial bond strength or adhesion of the coating to the substrate is a very important property of thin, hard coatings. Poor adhesion leads to "flaking" (adhesive failure), whereas poor cohesion causes chipping (cohesive failure). Adhesion can be evaluated by various techniques some of which, however, have serious limitations. Among them, the "scratch test" first proposed by Heavens[14] and introduced by Benjamin et al.[15] has led to consistently meaningful results and is applicable as a quality control tool in the production of large numbers of parts. They applied this method to soft coatings using other criteria for failure than those pertinent to hard coatings. They analyzed the scratch test in detail and showed that the action of the stylus involves plastic deformation of the substrate and that this deformation generates a shearing force at the film/substrate interface around the rim of the indentation produced by the point. This shearing force or adhesion was expressed in terms of tip radius, radius of the circle of contact, indentation hardness of the substrate material, and critical load which was defined as the minimum force applied to the stylus that stripped the film cleanly from the substrate leaving a clear channel.[14-16] Ahn et al.[17] established that: (1) a thin film, such as gold on glass, may get detached before formation of a cleared track and, conversely, an originally clear film may be made optically translucent without being removed; (2) the form of the track depends upon the relative hardness of the film and substrate; (3) stylus

6. THORNTON, J. J. Ann. Rev. Mater. Sci., v. 7, 1977, p. 239.
7. HINTERMANN, H. E. J. Vac. Sci. Technol., v. B2, no. 2, 1984, p. 81.
8. LINIAL, V., and HINTERMANN, H. E. Proceedings of the Conference on Wear of Materials, K. C. Ludema, W. A. Glaeser, and S. K. Rhee, ed., ASME, 1979, p. 403.
9. HINTERMANN, H. E. *Tribol. Int.* v. 13, 1980, p. 267.
10. HABIG, K. H., EVERS, W., and HINTERMANN, H. E. *Z. Werkstoffiech.* v. 11, 1980, p. 182.
11. HINTERMANN, H. E. *Thin Solid Films.* v. 8a, 1981, p. 215.
12. HINTERMANN, H. E., BORING, H., and HANNI, W. *Wear.* v. 38, 1978, p. 225.
13. MAILLAT, M., BORING, H., and HINTERMANN, H. E. Proceed. of the Space Tribology Workshop, Risley, GB, v. 3, 1980.
14. HEAVENS, O. S. J. Phys. and Rad., v. 11, 1950, p. 355.
15. BENJAMIN, P., and WEAVER, C. *Proc. Royal Society.* v. A 254, 1980, p. 163.
16. OROSHNIK, J., and CROLL, W. K. in *Adhesive Measurements of Thin Films, Thick Films and Bulk Coatings.* K. L. Mittal, ed., ASTM STP 640, ASTM, 1978, p. 158.
17. AHN, J., MITTAL, K. L., and MACQUEEN, R. H. in *Adhesive Measurement of Thin Films, Thick Films and Bulk Coatings.* K. L. Mittal, ed., ASTM STP 640, ASTM, 1978, p. 139.

size, film thickness, and surface finish determine whether failure occurs first in the film, the substrate, or at the interface; and (4) film detachment often occurs at loads lower than that required for track clearance which appears to depend on film tearing, film pile-up in front of the stylus, surface dust, and imperfections. The subjectivity of the complete removal criterion led to doubts regarding the quantitative reliability of the scratch test as a measure of thin film adhesion.[16,18] It was always observed[18] that at stylus loads well below the "critical load" there was some film detachment in spots, in the central portion of the track. Such observations led to the concept of "threshold adhesion failure" (TAF)[16] which occurs if, within the boundaries of a scratch and over its 1-cm path, removal of the film from its substrate can be detected by transmitted light with a microscope at 40X at even one spot, no matter how small. Each stylus exhibits its own individual scribing and testing characteristics. The TAF mean loads of one thin film sample can be compared with another or with a "standard," provided that for all measurements, the same stylus was used in the same position in the instrument. If the TAF determination is to be valid, stylus loadings should not exceed those levels at which crescent formation of the substrate will occur.

In scratch testing, stresses are introduced at the interface by deforming the surface with a moving diamond tip (r = 200 μm, angle 120°). The applied load is increased stepwise or continuously until the deformation causes stresses which result in flaking or chipping of the coating. The smallest load at which the coating cracks (cohesive failure) or is detached (adhesive failure) is called the critical load and is determined by optical or electron microscopy, as well as by acoustic emission (AE). Usually, the onset of AE signal and the microscopical observation of the first damage occurring in the coating correlate quite well. With the CSEM-Revetest, the scratches are made at constant translational speed and linearly increasing load with automatic recording of an AE-normal loading graph.

The purpose of this work was to use this automatic scratch testing apparatus in order to compare the quality and soundness of various coatings, as well as to measure their adhesive strength to a given substrate.

EXPERIMENTAL PROCEDURE

The following types of specimens prepared by various processes were used in this investigation: TiB_2-coated MP35N nickel-base alloy specimens; TiN-coated PH 17-4 steel specimens; and PH 17-4 steel specimens coated with a ternary Al_2O_3-SiO_2-Cr_2O_3 oxide.

Specimen Preparation

TiB_2-coated MP35N specimens were prepared by a fused salt electroplating process using a ternary eutectic electrolyte of LiF-NaF-KF (FLINAK) melting at 454°C, with titanium hexafluoride (TiF6) and boron hexafluoride (BF6). The electrodeposition temperature was 600°C.

The TiN-coated samples of PH 17-4 steel were prepared by two different vendors using two different cathodic arc PVD processes. The advantages of the arc evaporation device are that no molten metal pool is generated and, thus, the source can be used in any orientation. Also, the evaporation rate is much higher than with a sputtering source. This process was mainly developed for coating tool and die steels, as well as carbide cutting and forming tools with wear resistant materials. In contrast, CVD involves a gaseous chemical reaction and

18. BUTLER, D. W., STODDART, C. T. H., and STUART, P. R. J. of Physics, (D), v. 3, 1970, p. 877.

requires elevated substrate temperatures (up to 1050°C) which can be detrimental to the dimensions and metallurgical structure of the components. PVD processes, which are more recent, involve vaporizing the coating material inside a vacuum chamber containing the parts to be coated. The process is excellent for parts with critical tolerances because the required substrate temperature is much lower, usually only 150°C to 500°C. For this TiN wear coating application, the cathodic arc PVD process uses multiple arc evaporators to vaporize the coating materials directly from the solid. The vapor energy level is high (50 eV to 150 eV) and the level of ionization is very high (80% to 95%). Hence, adhesion is superior. The two vendors employed different equipment and sets of process variables producing type I and type II specimens.

The (Al_2O_3-SiO_2-Cr_2O_3) wear resistant coating was deposited by a CVD batch process on PH 17-4 steel specimens at a temperature of approximately 1000°C and a rate of approximately 0.5 μm/h. Deposition was followed by heat treatment to reharden the substructure.

Another type of specimen used herein consisted of SiC-coated 4340 low alloy steel. The SiC coatings were processed through decomposition of silane (SiH_4) and ethylene (CH_2=CH_2) in an RF discharge. The coatings, designated as a-SiC:H, invariably contained H_2 and had nominal Si/C ratios of unity, as detected by x-ray photoelectron spectroscopy (XPS). These coatings were partially or totally amorphous. As entrapped hydrogen diffuses out of the coatings, resultant shrinkage causes tensile residual stresses in the deposit. It is well established that at elevated substrate temperatures, less hydrogen is incorporated in the coatings. Accordingly, coatings deposited at elevated temperatures can better retain the compressive stresses generated by ion bombardment than those at low substrate temperatures. Coatings of 0.2, 0.4, and 0.75 μm were processed by applying 25 W to the substrate electrode at an ion bombardment energy of 90 eV.

Specimen Testing

The soundness and quality of various coatings were evaluated primarily with a CSEM-Revetest automatic scratch testing apparatus, Figure 1a, coupled with an X-Y chart recorder (LINSEIS) with an input impedance Ri > 5 K ohm and a sensitivity range S > 1 mV/cm. The apparatus includes: a diamond indenter with an original tip radius of 0.2 mm, a resonant acoustic emission detector (Bruel & Kjaer, Denmark) with an AE preamplifier and amplifier, an AE signal converter, a load cell, a load driving motor, a sample table with a driving motor, and a screw drive for manual lateral sample stage displacement. Two proximity switches limit the end of the stroke of the sample table and two others limit the end of the stroke of the loading device. Pen lift of the chart recorder can be achieved either automatically or manually directly from the control unit.

The testing procedure may be summarized as follows: The diamond point first comes down until it touches the surface of the sample. Then the normal load (force Fn) applied to the diamond immediately starts to increase linearly with time and its instantaneous value is displayed. During the motion of the table, the upper load display (min.-max.) flickers. When this force exceeds the preselected lower load, the sample starts to move and continues until the applied force reaches the desired upper limit load. Then the diamond is lifted up from the sample surface and the table moves back automatically to its original position so that after lateral translation, the equipment is ready for the next test. The adjustable variable load test parameters are: force range 1 N to 200 N, load display 100 div (full scale = 100/200 N), sample table translation speed 10 mm/min, and loading rate 100 N/min. Scratch

testing is also possible under constant load applied to the diamond point enabling scratching within the coating, at the coating/substrate interface, or within the substrate.

The abrasive wear resistance of type I and type II TiN coatings, as well as TiB_2 and (Al_2O_3-SiO_2-Cr_2O_3) were evaluated with a pin-on-disk apparatus,[19] Figure 1b. The disk was covered with commercial abrasive paper (grit grade 600 of about 12.4 μm average particle size) and was fastened to a turntable. The specimen had a stepped shaft configuration with a pin diameter of 0.00304 m. With the pin lowered onto the rotating abrasive paper disk, a static weight was added to the holder. The total normal force was F_n = 2.709 N or an average normal stress $P_n = F_n/A$ = 0.372 MPa. The tests were performed in air. The rotational velocities were set with a stroboscope at 50 rpm and 100 rpm, corresponding to tangential velocities of 0.217 m/s and 0.434 m/s, respectively. The rotational motion was terminated after various times from 10 to 345 min. Each test was interrupted often to change the paper and weigh the sample so as to eliminate, as much as possible, the effect of carbide particle wear on specimen specific wear rate.

Specimen cross sections were examined metallographically to determine film thickness and uniformity, as well as the presence of porosity or other discontinuities. The surface of coatings and the scratch track morphology were examined by scanning electron microscopy (SEM).

RESULTS AND DISCUSSION

In an acoustic emission versus load curve during a variable load scratch test, Figure 2a, the first acoustic event at L_C (load for cohesive failure) corresponds to the crack initiation within the coating. The slope of the curve abruptly increases at L_A (load for adhesive failure) which corresponds to the propagation of the crack at the coating-substrate interface, causing delamination. Results of scratch testing combined with micrographic observations may be summarized as follows.

TiB_2-Coated MP35N Specimens

A photomicrograph of a cross section of a coated specimen is shown in Figure 3a. The coating thickness, not very uniform, varies between 7 μm and 10 μm and some amount of microporosity is apparent. The results of the scratch test at variable load between 0 N and 70 N are exhibited in Figure 2a, where the acoustic emission signal intensity (arbitrary units), the tangential or friction force, F_t (N), and the friction coefficient, μ^*, have been plotted versus normal load, F_n (N). The AE curves show that cohesive failure occurs at a load L_C = 7 N and adhesive failure occurs at L_A = 28 N. The friction coefficient gradually increases with load from approximately 0 to 0.75 because of increasing penetration of the diamond point. The same parameters (AE, F_t, and μ^*) have been plotted in Figure 2b at constant load versus time. Selected loads were: 4 N (below L_C), 6 N (about equal to L_C), 10 N (above L_C) for which the scratch lies entirely inside the coating, and 29 N (above L_A) for which the scratch penetrates into the substrate. At a load of 4 N, there is no acoustic emission because the corresponding stress is below the yield point of the coating material.

19. CHEN, M., KATTAMIS, T. Z., CHAMBERS, B. V., and CORNIE, J. A. in *Engineered Materials for Advanced Friction and Wear Applications.* F. A. Smidt and P. J. Blau, ed., Conference Proceedings, ASM International, 1988, p. 63.

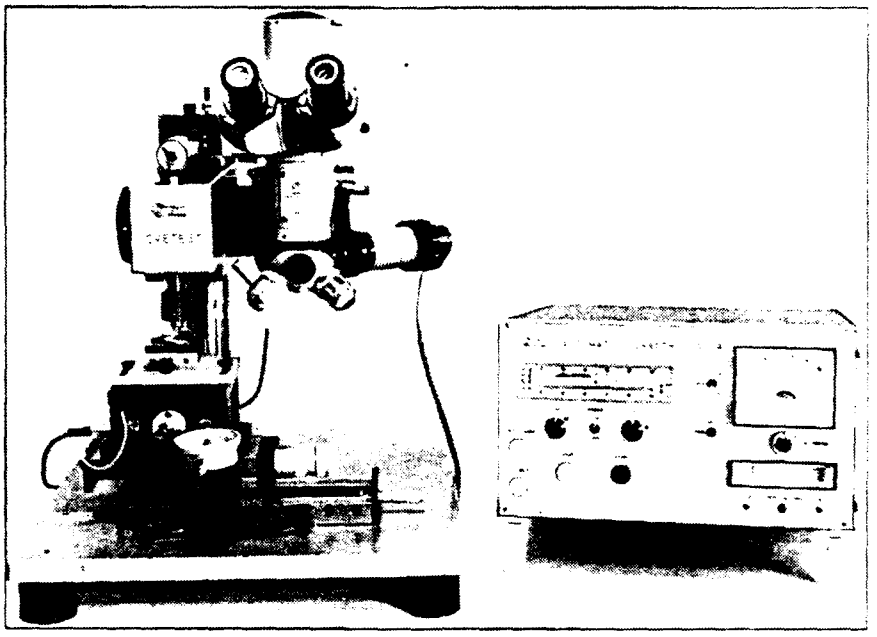

(a)

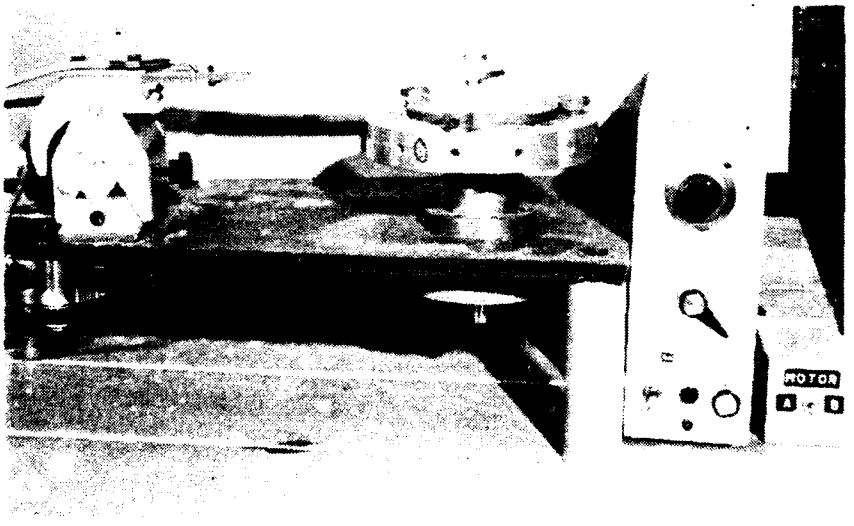

(b)

Figure 1. Photographs of (a) overall view of the CSEM-Revetest automatic scratch tester and (b) pin-on-disk apparatus used in evaluating abrasive wear resistance.

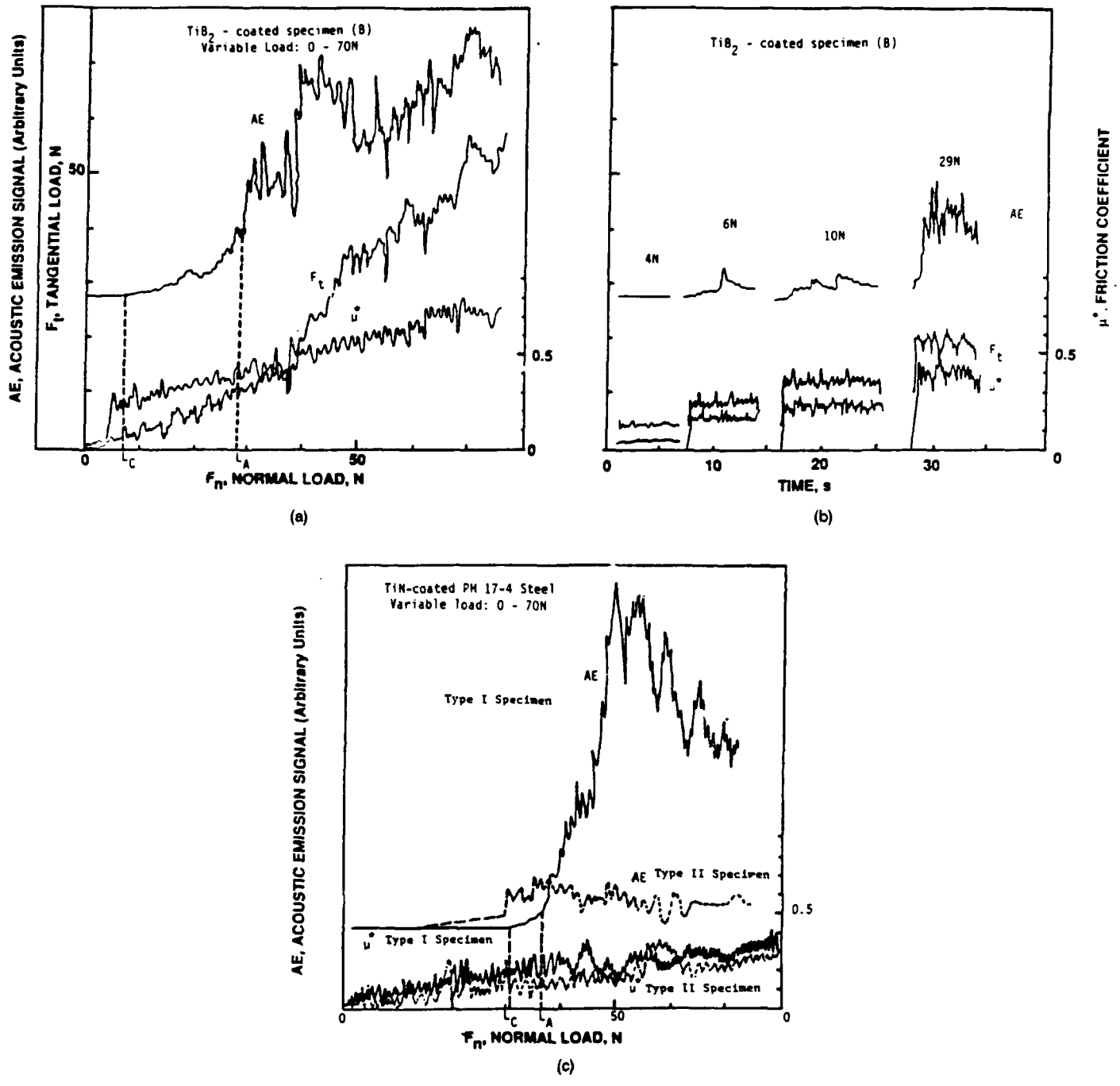

Figure 2. Acoustic emission signal (AE, arbitrary units), tangential or frictional load and friction coefficient versus normal load: (a) variable between 0 N and 70 N or (b) versus time at various constant loads for TiB_2-coated MP35N nickel-base alloy. (c) Acoustic emission signal and friction coefficient versus normal load variable between 0 N and 70 N for TiN-coated PH 17-4 steel, types I and II.

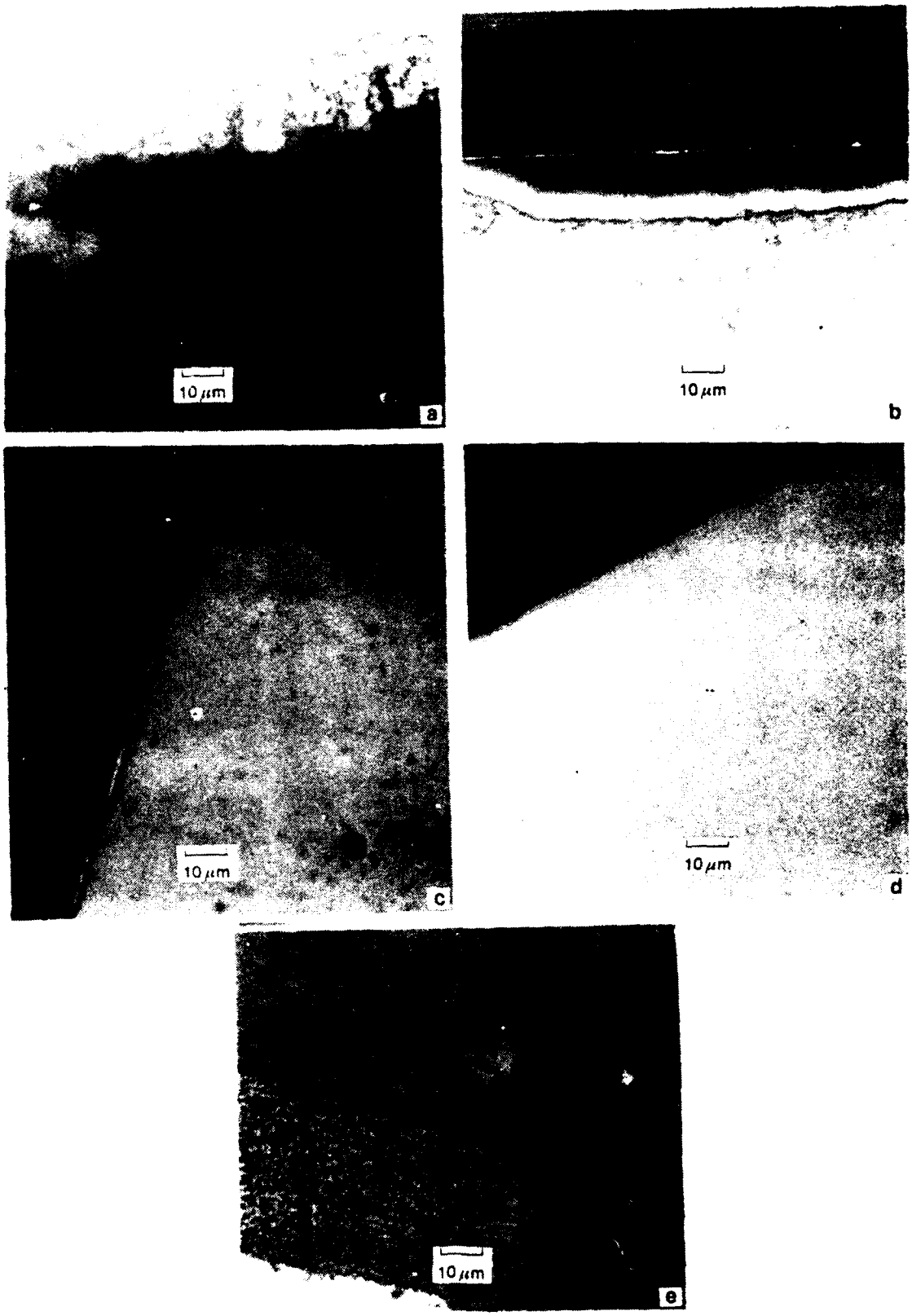

Figure 3. Photomicrographs of cross sections of various coated specimens: (a) TiB_2-coated MP35N nickel-base alloy, (b) TiN-coated PH 17-4 steel, (c) type I, etched with picral, (d) TiN-coated PH 17-4 steel, type II, and (e) (Al_2O_3-SiO_2-Cr_2O_3)-coated PH 17-4 steel.

Figures 4a through 4d are scanning electron micrographs illustrating the morphology of the scratch obtained under variable load (0 N to 70 N). A top view of the virgin coating is illustrated in Figure 4a and scratch morphology is shown in Figures 4b through 4d. Figure 4b corresponds to the beginning of the scratch and to a load of 35 N to 40 N. Some remaining islands of the film are still visible on the nickel-base substrate. Figure 4c corresponds to the middle of the scratch and to a load of approximately 50 N to 55 N. All the film has been removed by now and crescent-shaped cracks appear on the substrate surface. Figure 4d illustrates the end of the scratch.

Measurements of abrasive wear resistance of various TiB_2-coated specimens by the pin-on-disk apparatus are reported as specific wear rate W_s ($mm^3/N \cdot m$) where $W_s = \Delta\tau/P_nL$, $\Delta\tau$ is thickness reduction (nm) measured metallographically on polished transverse sections, and L is sliding distance (m). In this expression, $L = 2\pi rNt$, N is rotations/min, r = 0.0415 m is the radius of the pin trajectory, and t is time. The specific wear rate is plotted versus sliding distance in Figure 5 for various specimens at 100 rpm. W_s is approximately constant until the coating is eliminated. It then increases very rapidly. The abrasive wear resistance of TiB_2-coated specimens is inferior to that of specimens with the other coatings.

TiN-Coated PH 17-4 Steel Specimens

Two different types of specimens, I and II, produced by different manufacturers were evaluated by scratch testing. A photomicrograph of a cross section of specimen I is illustrated in Figure 3b. The coating thickness of about 2 μm is uniform and the coating-substrate interface appears to be sound; hence, adhesion is expected to be good. In Figure 2c, the AE responses of both specimens and the friction coefficients, μ^*, have been plotted versus normal load, F_n, which varied between 0 N and 75 N. For specimen I, L_C = 31 N and L_A = 37 N. For specimen II, both the cohesive and adhesive failure loads were substantially lower. The friction coefficient, μ^*, at a normal load of 20 N is approximately 0.3 for both specimens. Figures 3c and 3d show that the coating on specimen II is also approximately 2 μm thick. The thickness is not uniform and the coating is locally discontinuous. The intensity of the AE signal for coating I is orders of magnitude greater than that of process II. Assuming that the AE intensity is an indication of the energy released in generating a crack, a higher AE intensity for coating I would indicate a relatively strong and defect-free coating. On the other hand, a low AE intensity for coating II would indicate a weak coating full of microdefects such as discontinuities and microporosity, as confirmed by the SEM micrograph of a scratch on this coating, Figure 6c. Accordingly, a comparison of AE data for the two types of TiN coatings reveals that product II is substantially inferior to product I. Absence of any distinct L_A and L_C values for coating II suggests that its cohesive strength is very low. It is clear that the friction coefficient for coating I is slightly higher than that for coating II. It is generally assumed that a lower friction coefficient is preferable for a higher abrasive wear resistance. However, in this case, caution is warranted. The coefficient of friction established by the scratch tester is, in fact, a scratching coefficient and is an indication of the energy transferred in scratching the diamond stylus against the substrate. If the coating is of poor quality, the energy required to destroy the coating and reach the substrate would be relatively low. In addition, if the coating contains microporosity, Figure 6c, the energy required to break it up and form wear debris would be less than that for a porosity-free coating. Accordingly, a lower friction coefficient is expected when debris is present. Figures 6a and 6b illustrate SEM micrographs of a scratch on type I TiN-coated PH 17-4 steel specimen performed with a variable load between 0 N and 70 N. They correspond to two locations at which the normal loads were 30 N to 35 N and 45 N to 50 N, respectively. In Figure 6a, longitudinal striations appear in the TiN coating. In Figure 6b, the remaining islands of TiN are clearly visible with a crescent-like arrangement. Figure 6c shows a SEM micrograph near the beginning of a scratch on type II

TiN-coated PH 17-4 steel specimen corresponding to a load of 10 N to 15 N. The TiN coating is already failing. In Figure 6d, corresponding to a load of 20 N to 25 N, the coating has already been eliminated at such a low load. Very fine TiN debris pushed to the side of the scratch are shown in this figure.

The specific wear rate is plotted versus sliding distance in Figure 5 for type I specimens at 100 rpm and type II specimens at 50 rpm. W_s is approximately constant until the TiN coating is eliminated. It then increases very rapidly. The abrasive wear resistance of type I specimens is about 10 times higher than that of type II.

(Al_2O_3-SiO_2-Cr_2O_3)-Coated PH 17-4 Steel Specimens

The cross section of this specimen is illustrated in Figure 3e. The coating is about 30 μm thick, uniform and continuous. Figure 7a shows for this coating and for a variable load test, between 0 N and 75 N, with L_C = 22 and L_A = 38 N that the friction coefficient gradually increases with increasing normal load to about 0.3, which is approximately equal to that of TiN. For a coating about 30 μm thick, internally stored elastic energy is expected to be very high and L_A is expected to be low. Accordingly, a high value of 38 N exhibited by this coating implies a sound and a good quality coating.

The abrasive wear of various coated specimens is plotted versus sliding distance in Figure 5. It is clear that the wear resistance of these specimens is slightly higher than that of type II TiN-coated specimens, but is inferior to that of type I.

PECVD SiC-Coated 4340 Steel Specimens

The AE signal intensity, the tangential or frictional load, and the friction coefficient were plotted in Figure 7b versus variable load between 0 N and 80 N, for a 0.75-μm-thick coating. In this case, L_C = 17 N and L_A = 33 N. They are both lower than that of TiN which shows that the latter is a superior coating. The friction coefficient of SiC, on the other hand, is comparable to that of TiN.

As a concluding remark, it must be emphasized that the interpretation of scratch adhesion test results is indeed very complex.[20] The critical load for failure of the coating depends on coating thickness, coating and substrate hardness and elastic modulus, friction between stylus and coating surface, and internal stress in the coating which is generated by thermal mismatch, lattice misfit, etc. Among these variables, the internal stress depends on coating thickness. Thus, thermal mismatch stresses usually decrease with increasing coating thickness, whereas lattice misfit stresses remain independent of it. By and large, as the coating thickness increases, the average internal stresses decrease, hence the critical load increases. It is possible to compare critical loads only for coatings for which all variables except one remain constant. The TiN I and II specimens examined have the same substrate. They also have the same thickness and exhibit the same friction coefficients. The established difference in critical loads between them may, therefore, be attributed to differences in hardness or other properties, due to differences in deposit soundness, and most likely internal stresses in the coatings. The superior quality of type I specimens established by the automatic scratch tester was also confirmed by abrasive wear resistance measurements.

20. BURNETT, P. J., and RICKERBY, D. *Thin Solid Films.* v. 154, 1987, p. 403.

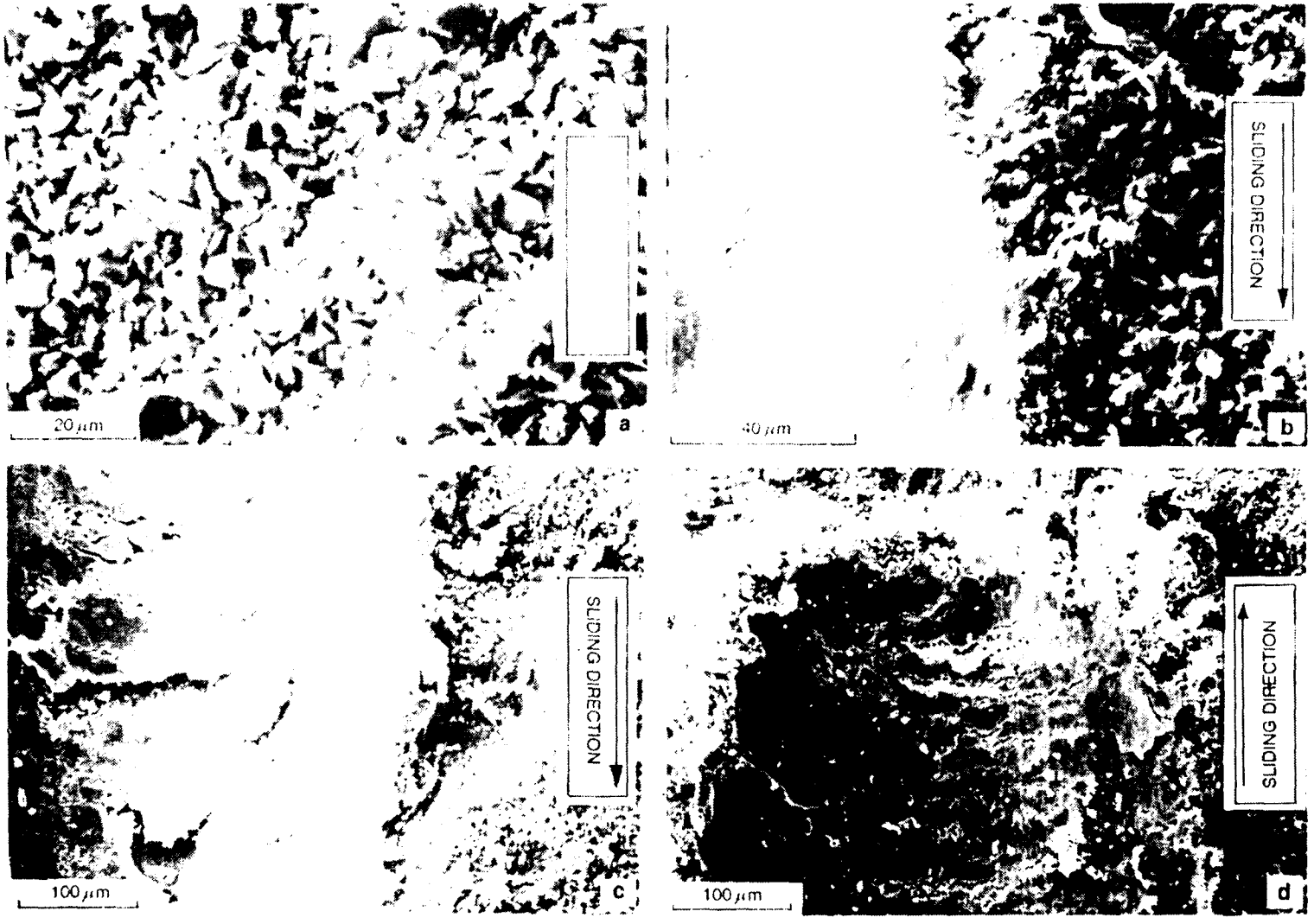

Figure 4. Scanning electron micrographs of the surface of (a) TiB_2-coated MP35N nickel-base alloy, and (b) of the scratch near its initiation, (c) middle, and (d) end.

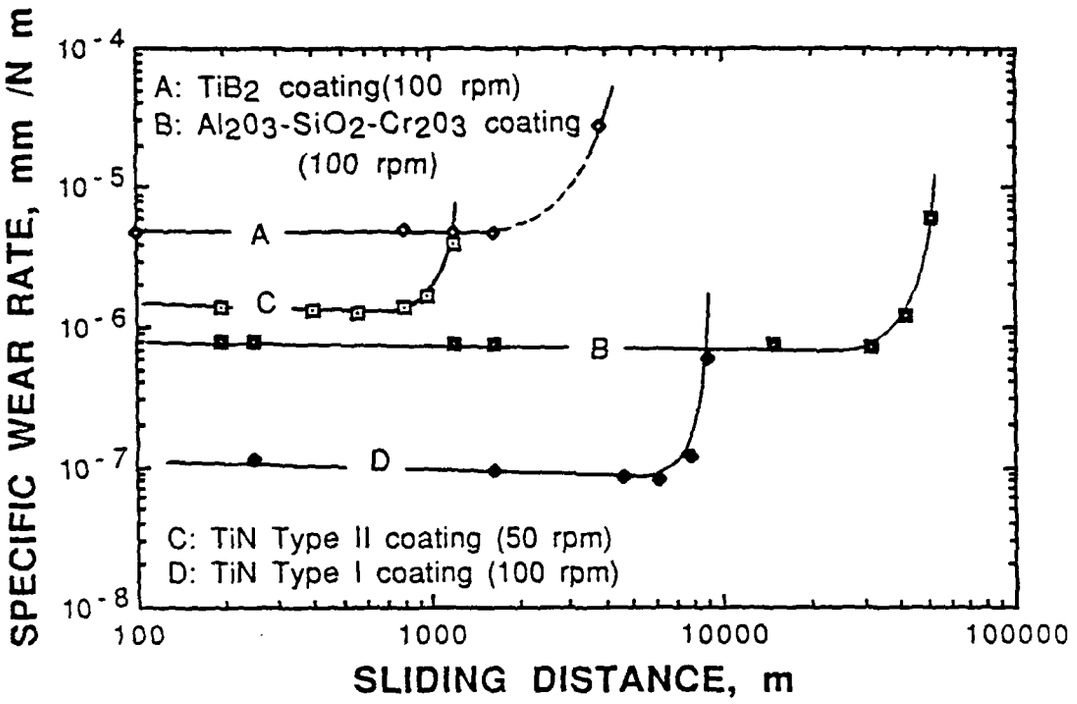

Figure 5. Specific wear rate versus sliding distance for various coatings.

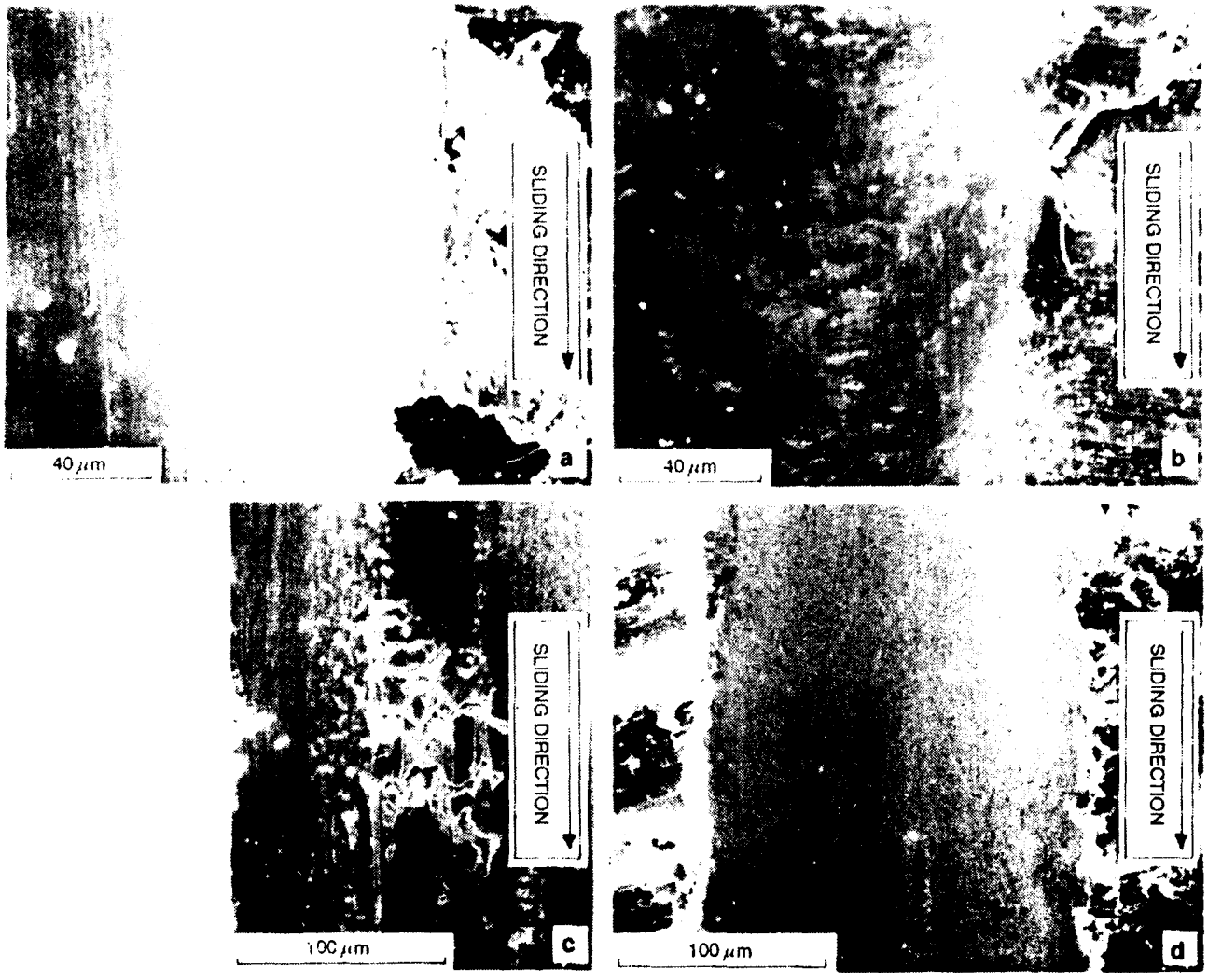

Figure 6. Scanning electron micrographs of scratches in TiN-coated PH 17-4 steel specimens. Micrographs (a) and (b) of type I specimen: (a) was taken near the beginning of the scratch (30 N to 35 N) and (b) farther away (45 N to 50 N); micrographs (c) and (d) of type II specimen: (c) was taken very near the beginning of the scratch (10 N to 15 N) and (d) slightly farther away (20 N to 25 N).

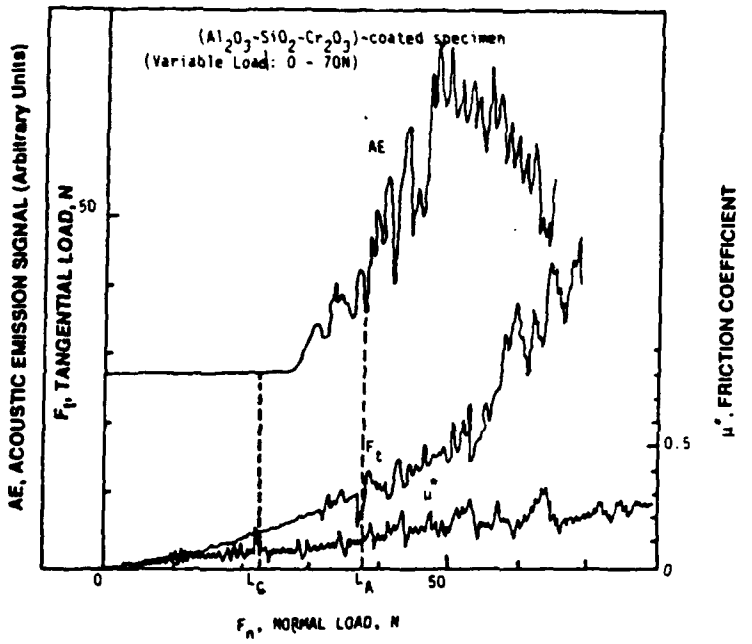

(a)

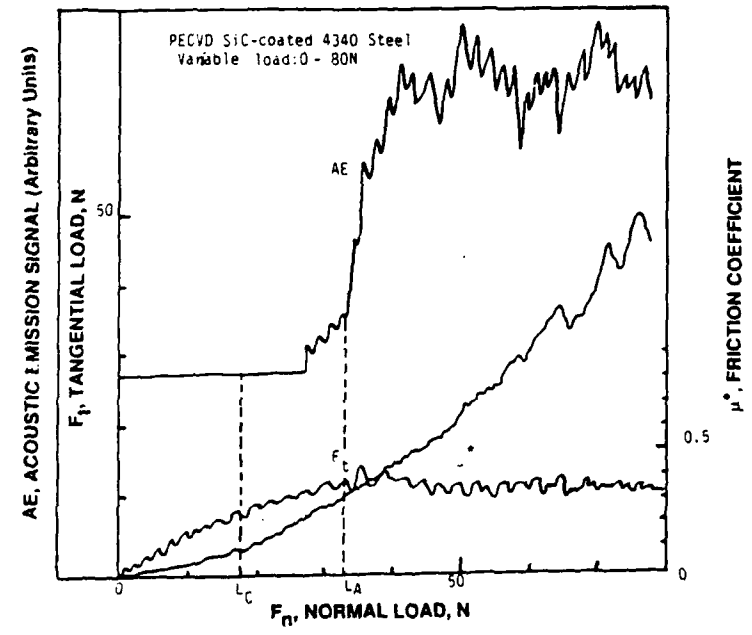

(b)

Figure 7. Acoustic emission signal (AE, arbitrary units), tangential or frictional load and friction coefficient versus variable load: (a) (Al_2O_3-SiO_2-Cr_2O_3)-coated PH 17-4 steel with variable load between 0 N and 70 N, *and* (b) PECVD SiC-coated 4340 low alloy steel, with variable load between 0 N and 80 N.

SUMMARY

The CSEM-Revetest automatic scratch testing apparatus was used for evaluating the quality and soundness of various coatings: TiB_2 on MP35N alloy, TiN on PH 17-4 steel, (Al_2O_3-SiO_2-Cr_2O_3) on PH 17-4 steel, and PECVD-processed SiC on 4340 low alloy steel. The scratch test gives the acoustic emission signal intensity, frictional or tangential force, and the scratching or friction coefficient versus load, or versus time at constant load. It was concluded that TiN-coated PH 17-4 steel specimens of type I exhibited higher cohesive and adhesive loads than the type II coated specimen or the other specimens tested, as well as a lower friction coefficient and a higher abrasive wear resistance, as confirmed by testing with a pin-on-disk apparatus. The intensity of the AE signal could be an indicator of the integrity of the coating.

DISTRIBUTION LIST

No. of Copies	To
1	Office of the Under Secretary of Defense for Research and Engineering, The Pentagon, Washington, DC 20301
	Commander, U.S. Army Laboratory Command, 2800 Powder Mill Road, Adelphi, MD 20783-1145
1	ATTN: AMSLC-IM-TL
1	AMSLC-CT
	Commander, Defense Technical Information Center, Cameron Station, Building 5, 5010 Duke Street, Alexandria, VA 22304-6145
2	ATTN: DTIC-FDAC
1	Metals and Ceramics Information Center, Battelle Columbus Laboratories, 505 King Avenue, Columbus, OH 43201
	Commander, Army Research Office, P.O. Box 12211, Research Triangle Park, NC 27709-2211
1	ATTN: Information Processing Office
	Commander, U.S. Army Materiel Command, 5001 Eisenhower Avenue, Alexandria, VA 22333
1	ATTN: AMCLD
	Commander, U.S. Army Materiel Systems Analysis Activity, Aberdeen Proving Ground, MD 21005
1	ATTN: AMXSY-MP, H. Cohen
	Commander, U.S. Army Missile Command, Redstone Scientific Information Center, Redstone Arsenal, AL 35898-5241
1	ATTN: AMSMI-RD-CS-R/Doc
1	AMSMI-RLM
	Commander, U.S. Army Armament, Munitions and Chemical Command, Dover, NJ 07801
2	ATTN: Technical Library
1	AMDAR-LCA, Mr. Harry E. Pebly, Jr., PLASTEC, Director
	Commander, U.S. Army Natick Research, Development and Engineering Center, Natick, MA 01760
1	ATTN: Technical Library
	Commander, U.S. Army Satellite Communications Agency, Fort Monmouth, NJ 07703
1	ATTN: Technical Document Center
	Commander, U.S. Army Tank-Automotive Command, Warren, MI 48397-5000
1	ATTN: AMSTA-ZSK
2	AMSTA-TSL, Technical Library
	Commander, White Sands Missile Range, NM 88002
1	ATTN: STEWS-WS-VT
	President, Airborne, Electronics and Special Warfare Board, Fort Bragg, NC 28307
1	ATTN: Library
	Director, U.S. Army Ballistic Research Laboratory, Aberdeen Proving Ground, MD 21005
1	ATTN: SLCBR-TSB-S (STINFO)
	Commander, Dugway Proving Ground, Dugway, UT 84022
1	ATTN: Technical Library, Technical Information Division
	Commander, Harry Diamond Laboratories, 2800 Powder Mill Road, Adelphi, MD 20783
1	ATTN: Technical Information Office
	Director, Benet Weapons Laboratory, LCWSL, USA AMCCOM, Watervliet, NY 12189
1	ATTN: AMSMC-LCB-TL
1	AMSMC-LCB-R
1	AMSMC-LCB-RM
1	AMSMC-LCB-RP
	Commander, U.S. Army Foreign Science and Technology Center, 220 7th Street, N.E., Charlottesville, VA 22901
1	ATTN: Military Tech

No. of Copies	To
	Commander, U.S. Army Aeromedical Research Unit, P.O. Box 577, Fort Rucker, AL 36360
1	ATTN: Technical Library
	Commander, U.S. Army Aviation Systems Command, Aviation Research and Technology Activity, Aviation Applied Technology Directorate, Fort Eustis, VA 23604-5577
1	ATTN: SAVDL-E-MOS
	U.S. Army Aviation Training Library, Fort Rucker, AL 36360
1	ATTN: Building 5906-5907
	Commander, U.S. Army Agency for Aviation Safety, Fort Rucker, AL 36362
1	ATTN: Technical Library
	Commander, USACDC Air Defense Agency, Fort Bliss, TX 79916
1	ATTN: Technical Library
	Commander, U.S. Army Engineer School, Fort Belvoir, VA 22060
1	ATTN: Library
	Commander, U.S. Army Engineer Waterways Experiment Station, P. O. Box 631, Vicksburg, MS 39180
1	ATTN: Research Center Library
	Commandant, U.S. Army Quartermaster School, Fort Lee, VA 23801
1	ATTN: Quartermaster School Library
	Naval Research Laboratory, Washington, DC 20375
1	ATTN: Code 5830
2	Dr. G. R. Yoder - Code 6384
	Chief of Naval Research, Arlington, VA 22217
1	ATTN: Code 471
1	Edward J. Morrissey, WRDC/MLTE, Wright-Patterson Air Force, Base, OH 45433-6523
	Commander, U.S. Air Force Wright Research & Development Center, Wright-Patterson Air Force Base, OH 45433-6523
1	ATTN: WRDC/MLC
1	WRDC/MLLP, M. Forney, Jr.
1	WRDC/MLBC, Mr. Stanley Schulman
	National Aeronautics and Space Administration, Marshall Space Flight Center, Huntsville, AL 35812
1	ATTN: R. J. Schwinghammer, EH01, Dir, M&P Lab
1	Mr. W. A. Wilson, EH41, Bldg. 4612
	U.S. Department of Commerce, National Institute of Standards and Technology, Gaithersburg, MD 20899
1	ATTN: Stephen M. Hsu, Chief, Ceramics Division, Institute for Materials Science and Engineering
1	Committee on Marine Structures, Marine Board, National Research Council, 2101 Constitution Ave., N.W., Washington, DC 20418
1	Librarian, Materials Sciences Corporation, Guynedd Plaza II, Bethlehem Pike, Spring House, PA 19477
1	The Charles Stark Draper Laboratory, 68 Albany Street, Cambridge, MA 02139
	Wyman-Gordon Company, Worcester, MA 01601
1	ATTN: Technical Library
	Lockheed-Georgia Company, 86 South Cobb Drive, Marietta, GA 30063
1	ATTN: Materials and Processes Engineering Dept. 71-11, Zone 54
	General Dynamics, Convair Aerospace Division, P.O. Box 748, Fort Worth, TX 76101
1	ATTN: Mfg. Engineering Technical Library
1	Mechanical Properties Data Center, Belfour Stulen Inc., 13917 W. Bay Shore Drive, Traverse City, MI 49684

No. of Copies	To
	Naval Research Laboratory 4670, Washington, DC 20375-5000
1	ATTN: Dr. Bruce Sartwell
	Argonne National Laboratory, Materials and Components Technology Division, Argonne, IL 60439
1	ATTN: Dr. G. R. Fenske
	Worcester Polytechnic Institute, Mechanical Engineering Department, Worcester, MA 01609
1	ATTN: Dr. Sarah Dillich
	Director, U.S. Army Materials Technology Laboratory, Watertown, MA 02172-0001.
2	ATTN: SLCMT-TML
2	Authors

U.S. Army Materials Technology Laboratory
Watertown, Massachusetts 02172-0001
QUALITY EVALUATION OF COATINGS
BY AUTOMATIC SCRATCH TESTING -
Kirit J. Bhansali and Theo Z. Kattamis

Technical Report MTL TR 89-98, November 1989, 18 pp-
illustrations

AD ____________
UNCLASSIFIED
UNLIMITED DISTRIBUTION

Key Words

Coatings
Ceramic coatings
Adhesion

The soundness and comparative quality of various coatings were evaluated with a CSEM-Revetest automatic scratch tester. These coatings were: TiB_2 on MP35N alloy, TiN on PH 17-4 steel, (Al_2O_3-SiO_2-Cr_2O_3) on PH 17-4 steel, and plasma-enhanced CVD-processed SiC on 4340 low alloy steel. During scratch testing, the acoustic emission signal intensity, the frictional or tangential force, and the friction coefficient were plotted versus load, as well as time at various constant loads. Scratch test results were correlated with coating microstructure which was investigated by optical and scanning electron microscopy (SEM). Significant difference in quality and soundness was detected for TiN coatings processed by two different methods. This difference was confirmed by abrasive wear resistance measurements.

U.S. Army Materials Technology Laboratory
Watertown, Massachusetts 02172-0001
QUALITY EVALUATION OF COATINGS
BY AUTOMATIC SCRATCH TESTING -
Kirit J. Bhansali and Theo Z. Kattamis

Technical Report MTL TR 89-98, November 1989, 18 pp-
illustrations

AD ____________
UNCLASSIFIED
UNLIMITED DISTRIBUTION

Key Words

Coatings
Ceramic coatings
Adhesion

The soundness and comparative quality of various coatings were evaluated with a CSEM-Revetest automatic scratch tester. These coatings were: TiB_2 on MP35N alloy, TiN on PH 17-4 steel, (Al_2O_3-SiO_2-Cr_2O_3) on PH 17-4 steel, and plasma-enhanced CVD-processed SiC on 4340 low alloy steel. During scratch testing, the acoustic emission signal intensity, the frictional or tangential force, and the friction coefficient were plotted versus load, as well as time at various constant loads. Scratch test results were correlated with coating microstructure which was investigated by optical and scanning electron microscopy (SEM). Significant difference in quality and soundness was detected for TiN coatings processed by two different methods. This difference was confirmed by abrasive wear resistance measurements.

U.S. Army Materials Technology Laboratory
Watertown, Massachusetts 02172-0001
QUALITY EVALUATION OF COATINGS
BY AUTOMATIC SCRATCH TESTING -
Kirit J. Bhansali and Theo Z. Kattamis

Technical Report MTL TR 89-98, November 1989, 18 pp-
illustrations

AD ____________
UNCLASSIFIED
UNLIMITED DISTRIBUTION

Key Words

Coatings
Ceramic coatings
Adhesion

The soundness and comparative quality of various coatings were evaluated with a CSEM-Revetest automatic scratch tester. These coatings were: TiB_2 on MP35N alloy, TiN on PH 17-4 steel, (Al_2O_3-SiO_2-Cr_2O_3) on PH 17-4 steel, and plasma-enhanced CVD-processed SiC on 4340 low alloy steel. During scratch testing, the acoustic emission signal intensity, the frictional or tangential force, and the friction coefficient were plotted versus load, as well as time at various constant loads. Scratch test results were correlated with coating microstructure which was investigated by optical and scanning electron microscopy (SEM). Significant difference in quality and soundness was detected for TiN coatings processed by two different methods. This difference was confirmed by abrasive wear resistance measurements.

U.S. Army Materials Technology Laboratory
Watertown, Massachusetts 02172-0001
QUALITY EVALUATION OF COATINGS
BY AUTOMATIC SCRATCH TESTING -
Kirit J. Bhansali and Theo Z. Kattamis

Technical Report MTL TR 89-98, November 1989, 18 pp-
illustrations

AD ____________
UNCLASSIFIED
UNLIMITED DISTRIBUTION

Key Words

Coatings
Ceramic coatings
Adhesion

The soundness and comparative quality of various coatings were evaluated with a CSEM-Revetest automatic scratch tester. These coatings were: TiB_2 on MP35N alloy, TiN on PH 17-4 steel, (Al_2O_3-SiO_2-Cr_2O_3) on PH 17-4 steel, and plasma-enhanced CVD-processed SiC on 4340 low alloy steel. During scratch testing, the acoustic emission signal intensity, the frictional or tangential force, and the friction coefficient were plotted versus load, as well as time at various constant loads. Scratch test results were correlated with coating microstructure which was investigated by optical and scanning electron microscopy (SEM). Significant difference in quality and soundness was detected for TiN coatings processed by two different methods. This difference was confirmed by abrasive wear resistance measurements.